electronics

MDPI

Article

Classification of Hand Movements Using MYO Armband on an Embedded Platform

Haider Ali Javaid [1,*], Mohsin Islam Tiwana [1], Ahmed Alsanad [2,*], Javaid Iqbal [1], Muhammad Tanveer Riaz [3,*], Saeed Ahmad [4] and Faisal Abdulaziz Almisned [5]

[1] Department of Mechatronics Engineering, College of Electrical and Mechanical Engineering, National University of Sciences & Technology, H-12, Islamabad 44000, Pakistan; mohsintiwana@ceme.nust.edu.pk (M.I.T.); j.iqbal@ceme.nust.edu.pk (J.I.)
[2] STC's Artificial Intelligence Chair, Department of Information Systems, College of Computer and Information Sciences, King Saud University, Riyadh 11451, Saudi Arabia
[3] Department of Mechanical, Mechatronics and Manufacturing Engineering, Faisalabad Campus, University of Engineering & Technology (UET) Lahore, Faisalabad 38000, Pakistan
[4] Department of Mechanical Engineering, College of Engineering and Technology, University of Sargodha, Sargodha 40100, Pakistan; saeed.aslam@uos.edu.pk
[5] Department of Information Systems, College of Computer and Information Sciences, King Saud University, Riyadh 11451, Saudi Arabia; falmisned@ksu.edu.sa
* Correspondence: haider.ali82@mts.ceme.edu.pk (H.A.J.); aasanad@ksu.edu.sa (A.A.); tanveer.riaz@ieee.org (M.T.R.)

Citation: Javaid, H.A.; Tiwana, M.I.; Alsanad, A.; Iqbal, J.; Riaz, M.T.; Ahmad, S.; Almisned, F.A. Classification of Hand Movements Using MYO Armband on an Embedded Platform. *Electronics* **2021**, *10*, 1322. https://doi.org/10.3390/electronics10111322

Academic Editors: Syed Aziz Shah, Qammer Hussain Abbasi, Jawad Ahmad and Muhammad Ali Imran

Received: 1 April 2021
Accepted: 11 May 2021
Published: 31 May 2021

Abstract: The study proposed the classification and recognition of hand gestures using electromyography (EMG) signals for controlling the upper limb prosthesis. In this research, the EMG signals were measured through an embedded system by wearing a band of MYO gesture control. In order to observe the behavior of these change movements, the EMG data was acquired from 10 healthy subjects (five male and five females) performing four upper limb movements. After extracting EMG data from MYO, the supervised classification approach was applied to recognize the different hand movements. The classification was performed with a 5-fold cross-validation technique under the supervision of Quadratic discriminant analysis (QDA), support vector machine (SVM), random forest, gradient boosted, ensemble (bagged tree), and ensemble (subspace K-Nearest Neighbors) classifier. The execution of these classifiers shows the overall accuracy of 83.9% in the case of ensemble (bagged tree) which is higher than other classifiers. Additionally, in this research an embedded system-based classification approach of hand movement was used for designing an upper limb prosthesis. This approach is different than previous techniques as MYO is used with an external Bluetooth module and different libraries that make its movement and performance boundless. The results of this study also inferred the operations which were easy for hand recognition and can be used for developing a powerful, efficient, and flexible prosthetic design in the future.

Keywords: electromyography (EMG); MYO gesture control; prosthesis; ensemble classifier

1. Introduction

Electromyography (EMG) is a diagnostic approach that use motor neurons to control and evaluate the health of muscles and neuron cells. These motor neurons are responsible for transmitting electrical signals through muscles to contract them. A lot of applications of EMG testing exists in clinical and biomedical fields. It can either be used as a diagnostic tool to locate the neuromuscular diseases or to control the prosthetic hand movement. Medical research denotes that different parts of forearm muscles and EMG signals related to hands and fingers can still be measurable even after the loss of the hand. Detection, analysis, and classification of the EMG signal is a well-known topic these days in the biomedical industry, especially in the case of prosthetic hand movement. For detection of EMG data from muscles, various invasive and noninvasive techniques are available [1].

In [2], the author proposed a unique method that controls the prosthetic hand using EMG signals produced by forearm muscle when hand and finger movement occurs. For measuring the sequence of EMG potential in this technique, EMG sensors were used with the help of a Personal Computer sound card. Eleven miniature electromagnetic sensors were mounted in this novel 3D electromagnetic positioning system along with a data-glove [3]. These 11 electromagnetic sensors had the capacity to capture the corresponding hand poses in a real-time scenario [4–6]. To collect the motor unit action potential (MUAP) on the skin area, highly reliable and responsive surface electromyogram (sEMG) electrodes were used in [7]. In [8], the author used SEMG sensors to carry out the EMG data for six healthy subjects. Two types of muscle contraction (isometric and isotonic) and (anisometric and anisotonic) were considered taking EMG data for applied forces. The surface electrodes show the limited ways to assess the muscular activity. In the case of sEMG, a pair of electrodes or a complex array of multiple electrodes would be used to record the muscle data. As EMG recording exhibits the potential difference between the two electrodes, that is why we need more than one electrode to capture data [9].

Intramuscular EMG electrodes also play a vital role in acquiring EMG data through various recording techniques. The monopolar needle electrode is one of the simplest approaches of intramuscular EMG electrodes consisting of fine wire to penetrate a muscle with a surface electrode as a reference outside [10]. Two wire monopolar needle electrodes are also used to inject in muscle for data acquisition concerning each other. These monopolar EMG electrodes are insulated and stiff enough to insert in the skin with the tip exposed to reference using surface electrodes. Most commonly, these intramuscular electrode fine wire recordings are used for research or in studies of kinesiology [11]. The change in the upper limb movement shows the vital change in amplitude and features of the surface electromyographic (sEMG) signals [12].

A three dimensional (3D) printed prosthesis used for below elbow amputees is paired with an MYO armband to provide an affordable, practical, and convenient solution for amputees [13,14]. The study of feature extraction is carried out from the acquired EMG data for normal and amputee subjects in time domain and frequency domain [15,16]. The approach of classification of hand movements for healthy subjects and to predict the same for amputees is under discussion in our study rather to extract time domain and frequency domain features that is a quite different mode of study. In [17], the author used the MYO armband with interfacing a developed app of MYO Analyzer that supports the movement of MYO with its own Bluetooth module. While, we used a different library of MYO Bridge with compatibility of an external BLE (Bluetooth-Low-Energy) HM-10 (Jinan Huamao Technology Co., Ltd., Jinan, China) and different movements than installed gestures of MYO armband as used in previous approach. Moreover, they did not mention the subjects and data segmentation while we used two different gender groups with variety of ages, vast data set and movement classification. In [18], the author basically compares both approaches of acquiring data from MYO and conventional EMG data acquisition system for pattern recognition. For this purpose, he used the classification phenomenon. In comparison with proposed approach, our study is very different in terms of data acquisition technique for MYO, classification of EMG data for various hand movements and the novelty of the embedded system for our mechanical design of the prosthesis.

Although the previous approaches improve the cost of amputation, it is still very expensive, particularly for the patients of underdeveloped countries. Therefore, the novelty in this study is to give a noninvasive, feasible and cost-effective solution for people with amputations. The paper presents an advancement in the embedded based classification approach of hand movements which has application in various control applications, especially upper limb prostheses and robotics. Additionally, this work addresses the issue of latency and accuracy in such applications which are a bottleneck in many of the current biomedical device applications. The approach that is adopted in this study is comparatively feasible and cheaper as compared to previous approaches as it uses the noninvasive simple device of the MYO armband which can be wearable on any size of muscle without

shuffling of wires, an embedded controller with low price and an HM-10 Bluetooth module for transmitting data. For further progress in the future, we can design a cost-efficient prosthetic upper limb to perform an action through this embedded system.

2. Background and Related Work

The electromyography (EMG) pattern recognition system acquired the EMG data from passive sensors, an innovative analog front-end system, and a power microcontroller to get different hand gestures. The data was acquired with the help of Cerebro AFE (Analog Front End IC for broadband communication) and fed into an MCU (microcontroller unit) [19]. In order to recognize the different hand gestures, the fed data was passed through the SVM classifier.

The author in [20] used the feature extraction methodology from the EMG data acquisition while we do not use the feature extraction methodology here. Our approach is just based on the classification of mentioned hand movements for the better performance of our mechanical design of prostheses. Moreover, this approach deals only with the features of amputees while we test the data of healthy subjects as well as to test for amputees. In [21], the author used a feature extraction-based methodology (time domain and frequency domain) that were extracted from raw EMG data to predict the behavior of hand gestures while we used the real time based raw EMG data classification of four movements without going into feature extraction methodology. Our one study of related feature extraction methodology was also published in ACM series publication with the name of "Comparative Analysis of EMG Signal Features in time domain and Frequency-domain using MYO Gesture Control". Finally, in [22] the author proposed the EMG data acquisition approaches with various set ups performing different gestures. The goal of their study to provide the best way of EMG data acquisition after classification phenomenon while in our case the stream of study is different as we want to develop an embedded system base classifier that predicts the future movement of an amputee with our undertaken mechanical design of prostheses.

For de-noising, classification and feature extraction, multiscale principle component analysis (MSPCA), a decision tree and discrete wavelet transform (DWT) was implemented, respectively, in [23,24]. This framework classified the EMG signal as taken by normal, myopathic and ALS (Amyotrophic lateral sclerosis) automatically with C4.5 algorithm, classification and regression tree (CART), and random forest decision tree classifiers. In [25], the author compared the classification performances of multilayer perception (MLP) and support vector machine (SVM). Surface electrodes obtained the EMG signals from the ulnar nerve of patients with DAQ (Data Acquisition) board and 16-bit A/D (Analog to Digital) converter which was stored in a computer's hard disk. The stored EMG data was then used for feature extraction using FFT (Fast Fourier Transform) and PCA (Principal Component Analysis). The PCA coefficients were applied to both MLP and SVM classifiers which show that SVM has a high rate of anticipation in diagnosing neuromuscular disorders.

To detect the wandering behavior of men/women through human recognition activity an approach of data mining was used in [26]. For this purpose, an MYO armband was used to capture the EMG data from muscles. The data obtained from volunteers then transferred to the computer wirelessly from MYO armband through a Bluetooth device. The MEX file of MATLAB (R2018b, Mathworks, Natick, MA, USA) was used to obtain data as MYO works in C/C++ but does not work in MATLAB. The 10-cross validation was used to recognize their motion activities using the frame of SVM, KNN, and naïve Bayes.

In [27], the author reveals the characteristics of different gestures via MYO armband and a gives a case study of an MYO armband that can use it to recognize gestures in map navigation with the help of Apple Maps Connector. In [28], the author proposed a comprehensive study for supervised classification of multichannel surface EMG signals. This representation shows the discrete wavelet transform (DWT) of EMG signals along with unconstrained parameterization of the mother wavelet [29–34]. The approach of support vector machine (SVM) is used to classify in a space of multichannel representation.

The results of this study show the discrimination of six hand gestures by getting a rate of 5% misclassification [35–38].

3. Proposed Methodology

The study in this paper involves the MYO armband with an embedded system to evaluate the EMG signals. For this approach, we interface our MYO armband to a controller board through an external HM-10 Bluetooth module. The proposed methodology block diagram is shown in Figure 1. The MYO armband is a manufactured product of Thalamic labs that can be used to detect the EMG signals of the forearm muscle. MYO contains eight EMG sensors to recognize the movement of arms and hand gestures. Besides these EMG sensors, MYO also has a nine-axis inertial measurement unit (IMU) to mark the hand movement. The IMU consists of a three-axis accelerometer, three-axis gyroscope, and three-axis magnetometers to account for the different movements. In our case, we used this device because it can be worn on any forearm due to its elasticity and wireless behavior.

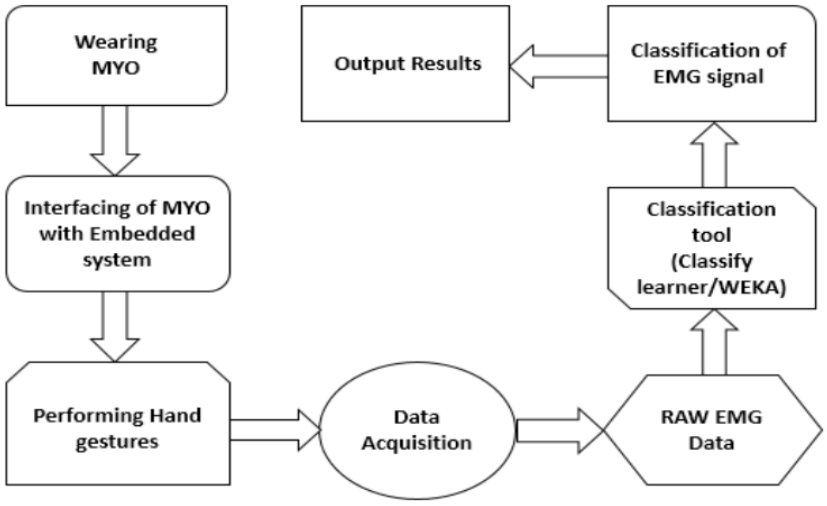

Figure 1. Proposed methodology block diagram.

There were 13 features of time domain and frequency domain selected in this research. These features were analyzed linearly and nonlinearly with specific parameters. Additionally, these features and attributes were used for classification of four-class hand gestures.

The time domain features consist of

- mean absolute value (MAV),
- variance of EMG signal (VAR),
- standard deviation (SD), skewness, kurtosis,
- standard error (SE),
- mean absolute deviation (MAD).

Likewise, the frequency domain features carry the attributes of

- mean frequency,
- median frequency,
- power bandwidth,
- total harmonic distortion (THD),
- signal to noise ratio (SNR),
- power spectral density (PSD) of signal.

3.1. Interfacing MYO with Arduino

A different embedded system can be utilized to interface the MYO armband, but in proposed approach, the Arduino UNO controller board is used to interface the MYO armband.

To access the raw EMG data, we used an external HM-10/CC2541 BLE Bluetooth module that must be flashed out with MyoBridge firmware before communicating to MYO as shown in Figure 2a. In order to make Arduino enabled for use with MYO, we used the library of MyoBridge that includes the EMG, IMU, and hand pose functions. The EMG data transfer rate is at 200 Hz while for IMU it comes out at 50 Hz. That is why in our dataset we obatined four times more EMG data than IMU data as shown in Figure 2b.

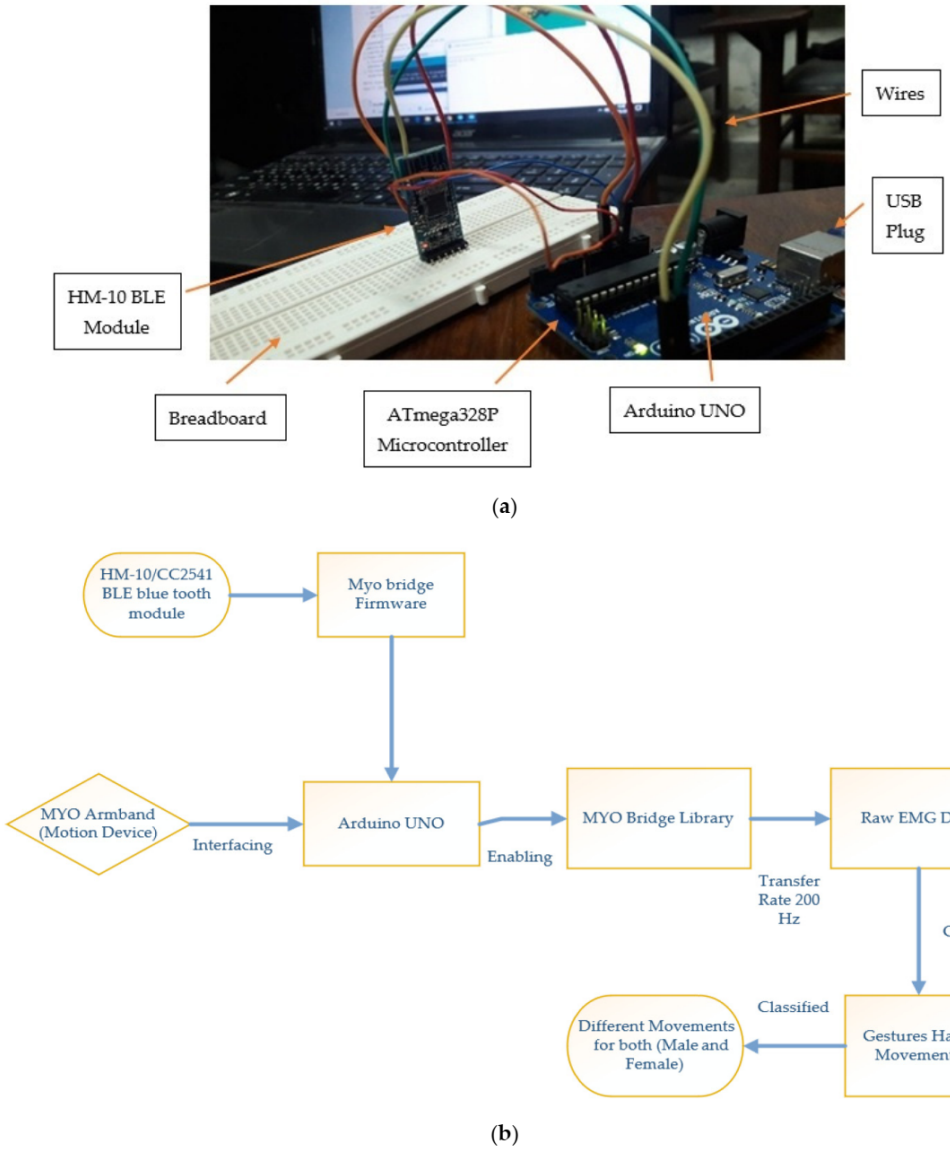

Figure 2. (**a**) Hardware interfacing of MYO. (**b**) Measurement system for eight-channel EMG (electromyography) and IMU (inertial measurement unit).

In this experiment, we selected five healthy male and five female subjects of different age groups (25–55 yr) to perform four hand movement gestures such as stationary, double-tap, single finger movement, and finger spread. These four gestures were further used to classify the different hand movements for both males and females separately. The EMG graph of the 8-channel MYO armband for different hand movements of males is shown in Figure 3.

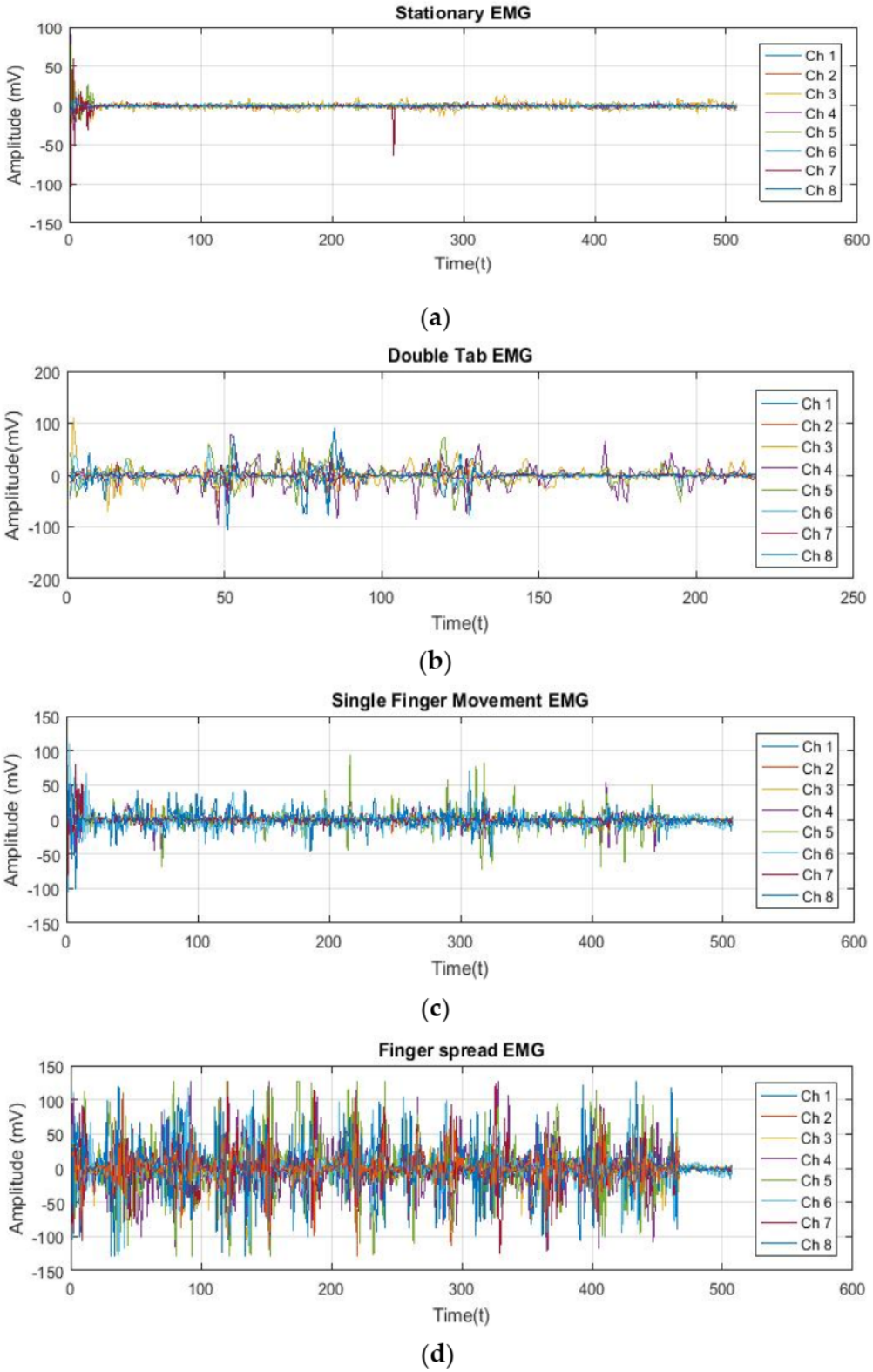

Figure 3. EMG graph of eight-channel MYO armband for male subjects. (**a**) Stationary EMG signal, (**b**) double tap EMG signal, (**c**) single finger movement EMG signal, and (**d**) finger spread EMG signal.

EMG signals are usually the product of motor unit action potentials (MUAPs) from various motor units. Different motor units have different MUAPs with change characteristic shapes and sizes. The size and shape of MUAPs depend upon the position of the electrode

or sensor with respect to muscle fibers and it can be changed with a moving electrode or sensor from its position.

The muscle tissues are normally inactive at rest as shown in Figure 3a. Whenever the muscle gets contracted voluntarily, the action potentials start to occur. Muscle fiber produces more and more action potential with the relatively increased strength of muscle contraction. That is why in Figure 3b,c the different orders of action potentials with increasing rates and amplitudes can be seen. Peaks with varying amplitude in Figure 3b show the motion of double tap with each double tap movement. Similarly, in the case of single finger movement as mentioned in Figure 3c, the normal contraction of muscle with orderly action potentials and smaller amplitude. When the muscle is fully contracted as in the case of finger spread, a group of action potentials from several motor units appear disorderly with higher rates and amplitudes as shown in Figure 3d. The same muscle activation for various hand movements can be seen in the female test group as well where stretching of tissues and peaks of action potentials shows the saturation in finger spread and single finger movement as shown in Figure 4.

3.2. Classification and Recognition of Hand Gesture

In this section, the classification approaches used for EMG signal classification are described. This system aims to classify the various hand movements with high accuracy rate. Figure 5 shows the study of four gesture EMG data plus stationary, double tap, single finger movement, and the finger spread. For this purpose, seven classifiers were used to classify our hand movements based on classification tools of WEKA, rapid minor and classify learners in MATLAB (R2018b).

3.3. Quadratic Discriminant Analysis (QDA)

Quadratic Discriminant Analysis (QDA) can be used for classifying or distinguishing the dimensions of two or more classes of objects within a surface quadrature. Quadratic Discriminant Analysis (QDA) is a very closely linked group of linear discriminant analysis (LDA), where it has been noticed that the dimensions from each class are normally dispersed. Though, in contrast to LDA, QDA has no postulation in which covariance of each of the classes is identical. When the normality postulation is true, the best conceivable test for the hypothesis that a given measurement is from a given class is the likelihood ratio test. As we mentioned that QDA is not very dissimilar from LDA except that you assume that the covariance matrix can be diverse for each class, therefore, we will estimate the covariance matrix Σ_k separately for each class k as k = 1, 2, . . . , K.

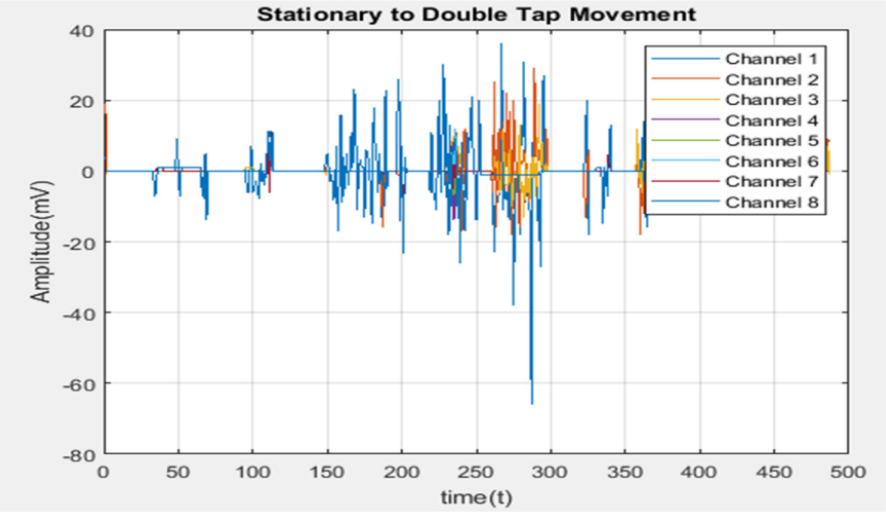

(a)

Figure 4. *Cont.*

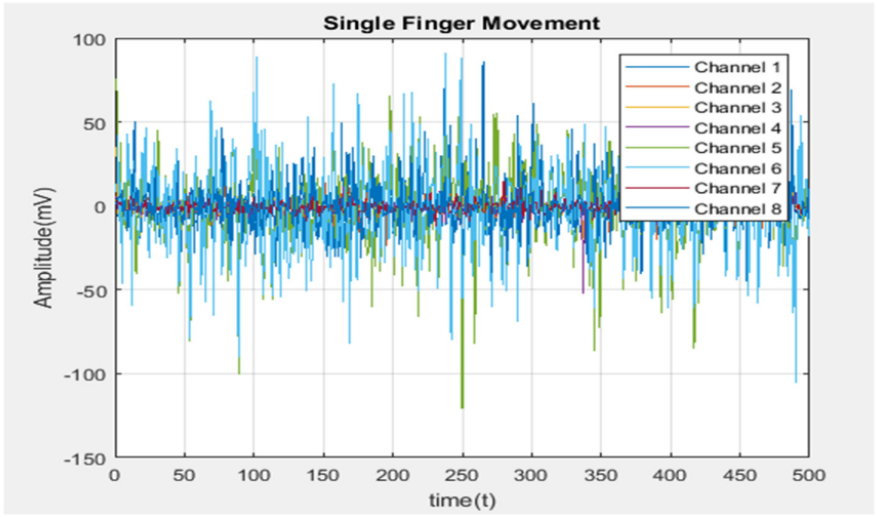

(**b**)

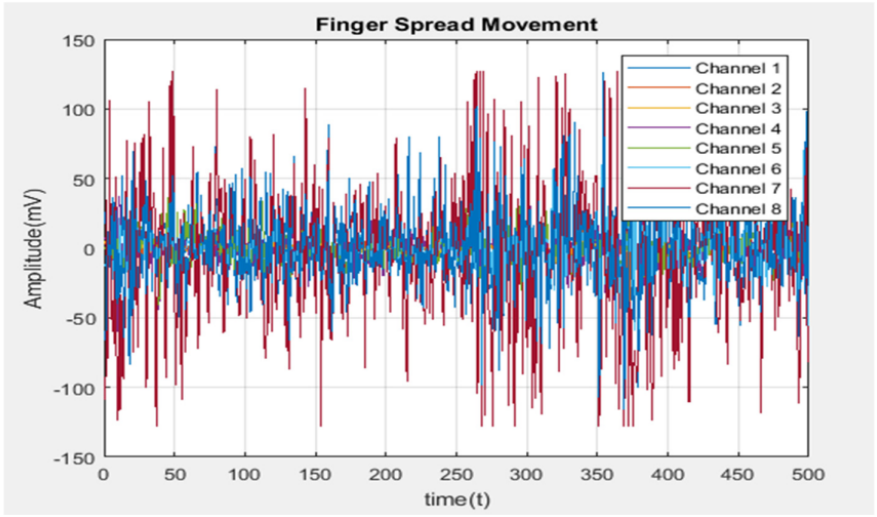

(**c**)

Figure 4. EMG graph of eight-channel MYO armband for female subjects. (**a**) Stationary EMG signal to double tap EMG signal, (**b**) single finger movement EMG signal, and (**c**) finger spread EMG signal.

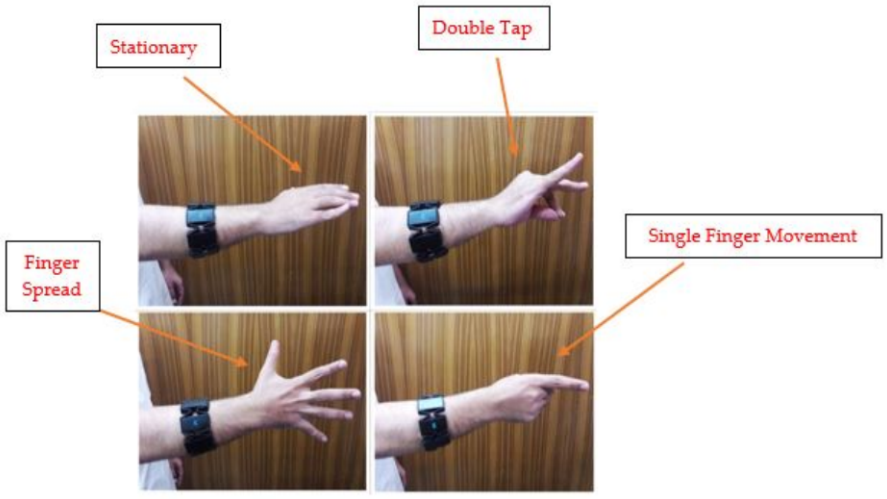

Figure 5. Four-gesture hand movement.

Quadratic discriminant function [12]:

$$\delta_k(x) = -\frac{1}{2}\log|\sum_K| - \frac{1}{2}(x-\mu_k)^T\sum_k^{-1}(x-\mu_k) + \log\pi_k \quad (1)$$

In Figure 6 the discriminant function is basically a second order classifier. The pattern of classification is parallel as well. You just bargain the class k which capitalizes on the quadratic discriminant function. The decision boundaries are quadratic equations in x.

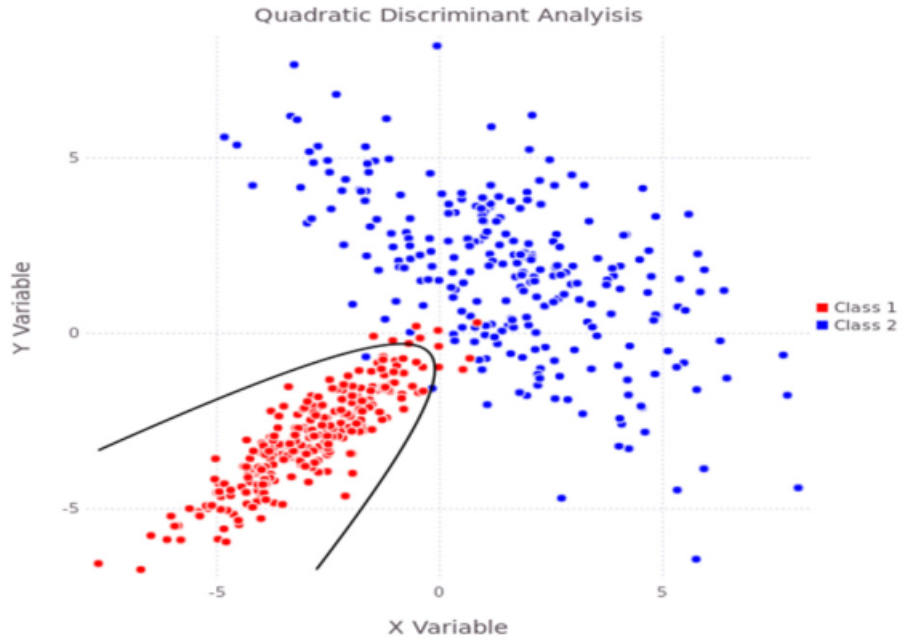

Figure 6. The quadratic discriminant analysis (QDA) function [12].

Classification rule:

$$\hat{Q}(x) = \text{argmax}\delta_k(x) \quad (2)$$

QDA has significantly more parameters than LDA because it has more litheness for the covariance matrix as it inclines to fit the data better than LDA. Therefore, for QDA assessment, you would have a discrete matrix of covariance for each class. If you have numerous classes and not enough sample points for it, then it will be problematic.

3.4. SVM Classifier

The support vector machine is basically a supervised learning model with specific learning algorithms used to compute the data for classification. In contrast with linear classification, SVM can also be used for nonlinear classification using the feature of kernel trick as shown in Figure 7.

A binary classifier is a function f: X → Y which nominates every point as x ∈ X with some y ∈ Y. Both linear SVM and quadratic SVM are based on kernel version classifiers.

$$f(x) = \sum_i \alpha_i y_i (x_i^T x) + b \quad (3)$$

where w > x + b = 0 and c (w > x + b) = 0 define the same plane [15]. We can choose the normalization of w for both cases as positive and negative support vectors. Choose normalization such that:

$$w^T x_+ + b = +1 \quad (4)$$

$$w^T x_- + b = -1 \quad (5)$$

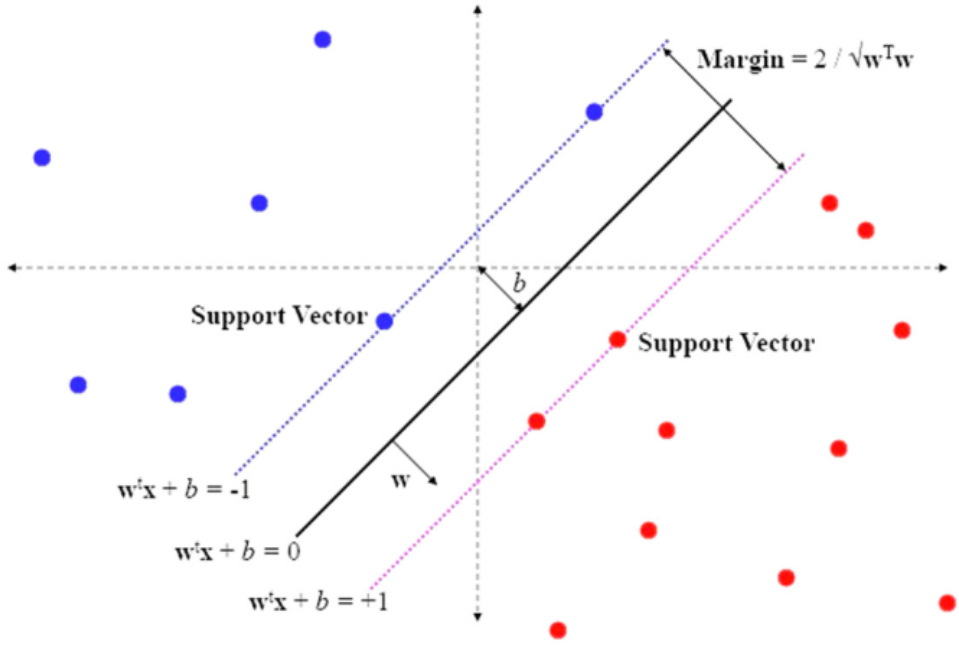

Figure 7. The graphical representation of SVM classifier [15].

Margin is given as:

$$\frac{w}{\|w\|}.(x_+ - x_-) = \frac{w^T(x_+ - x_-)}{\|w\|} = \frac{2}{\|w\|} \tag{6}$$

The learning algorithm of SVM can be formulated as:

$$\max_w \frac{2}{\|w\|} \text{ subject to } w^T x_i + b \begin{array}{ll} \geq 1 & if \quad y_i = +1 \\ \leq -1 & if \quad y_i = -1 \end{array}$$

for $i = 1 \ldots N$

$$\min \|w\|^2 \text{ subject to } y_i(w^T x_i + b) \geq 1 \text{for } i = 1 \ldots N$$

3.5. Ensemble (Bagged Tree)

An ensemble classification method is a supervised learning approach that synthesizes the multiple predictions of various machine learning algorithms together in order to get the better prediction than a single algorithm. Bagging or bootstrap aggregation can be used to train data for prediction and to reduce the variance of high variance algorithms like classification and regression tree (CART). Decision trees are very sympathetic and acute towards trainee data. If any changes occur in training data, then it also affects the resulting decision trees which in turn change the results of prediction. In the case of bagged decision trees, we are less apprehensive toward the single tree overfitting the trainee data. For efficiency and higher accuracy, the single decision trees should grow deep with each leaf-node containing a few trainee samples as shown in Figure 8.

For classification or regression of data we have

$$(Xi, Yi)\ (i = 1, \ldots, n),$$

where Xi ∈ IRd mentions the d-dimensional predictor variable and the response Yi ∈ IR (regression) or Yi ∈ {0, 1, J − 1} (J-class classification).

For regression the target function is IE [Y | X = x] and for classification of multivariate functions it should be:

$$\text{IP } [Y = j \mid X = x]\ (j = 0, J - 1)$$

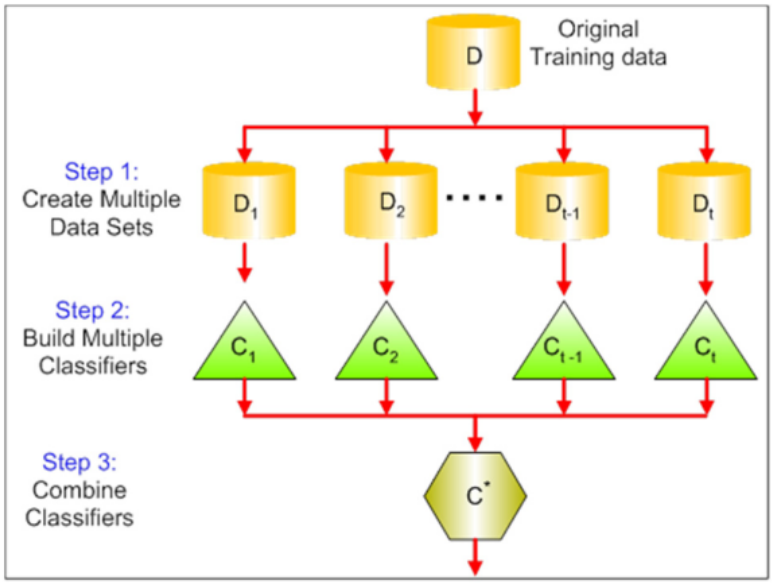

Figure 8. A model of ensemble (bagged tree) [20].

The function estimator which in turn is the result of the base procedure is given as:

$$g(\cdot) = hn((X1,Y1), \ldots, (Xn,Yn))(\cdot): IRd \rightarrow IR, \quad (7)$$

The variables for the bagged trees algorithm only include the number of samples and the number of trees to count. Models that have large data take time for training, but it will not follow the overfitting in training data.

3.6. Gradient Boosted (Tree)

Gradient boosted is a method that also exists to perform the different supervised machine learning tasks i.e., classification and regression just like the random forests (RF) method. The implementation of this technique is very easy and recalled as with different names. The most common name is gradient boosting machines (GBM) and XGBoost. It is an ensemble learner the same as RF that creates an end model based on the collection of individual models. It has very weak power as an individual model but when these individual models (weak power) combine as a group, it provides a better-quality result. A commonly used type of weak model in GBM is a decision tree as shown in Figure 9.

In boosting, individual models i.e., weak learners are not just built by random subsets of data and features except that it also puts some more weight in the form of incorrect predictions and highly faulty data for the better training. In this way, these models learn in a better way from previous errors/mistakes. This type of boosting is upgraded with a name called stochastic gradient boosting (SGB) in which each ensemble trains with a subset of data. This provides the most generalized and improved model for results.

Minimization of the loss function is done with gradient, in which neural networks are trained by using gradient descent for optimization of the weights. For the training of this model, the weak learners are built, and their predictions are compared with the correctly obtained results. Error rate of this model is defined as the distance between prediction value and its true (correct) value. Therefore, these errors find the gradient. It is simply a derivative of the given loss function. It also provides a direction in which errors of the model can be reduced by "descending the gradient" for the next step of training.

In this case a gradient descent is implemented in order to calculate the learning rate (descending the step size of the gradient), shrinkage (decreasing the learning rate) and loss function used as hyperparameters in GBM.

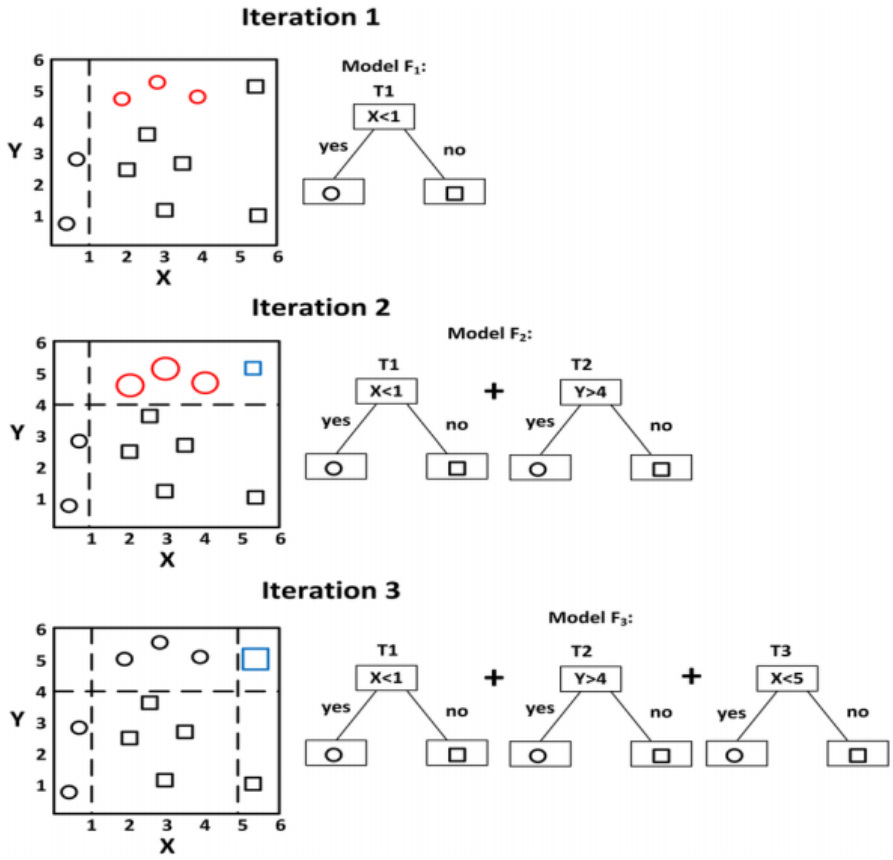

Figure 9. Features of gradient boosted (tree) [20].

Algorithm: In many supervised learning problems, there is an output variable y and a vector of input variables x described through a joint probability distribution $P(x, y)$. Using a training set $\{(x1, y1), \ldots, (xn, yn)\}$ of known values of x and corresponding values of y, the goal is to find an approximation of a function $F(x)$ that minimizes the expected value of some specified loss functions $L(y, F(x))$ [20].

$$\hat{F} = \underset{F}{\operatorname{argmin}} E_{x,y}[L(y, F(x))] \tag{8}$$

3.7. Random Forest

Random forest is the improved version of bagged decision trees. The combined effect of multiple predictions from various models can give a better prediction rate from the uncorrelated sub models or weakly correlated models of prediction. In the decision trees algorithm, a problem arises especially in CART that they are greedy algorithms, so they pick a variable to split through the greedy algorithm to minimize the error. There are a lot of similarities in pattern and design configuration for decision trees in case of a bagged tree and they have a high correlation in their prediction level. While in the case of the random forest shown in Figure 10, they changed the algorithms as sub-trees learned in their training process, so their resulting predictions have less correlation among these sub-tresses. The algorithm used for training in the case of random forest applies the same approach as used by bagging or bootstrap aggregation trees to learn. If the data set is given as:

X = x1, . . . , xn with responses Y = y1, . . . , yn, bagging to select a random sample of trainee data and try to fit trees to these samples: For b = 1, . . . , B:

Where sample with replacement, B training examples from X, Y represent as Xb, Yb and train a decision or regression tree fb on Xb, Yb. Then, after training, predictions of unseen data can be achieved by computing the prediction average of individual trees on x′.

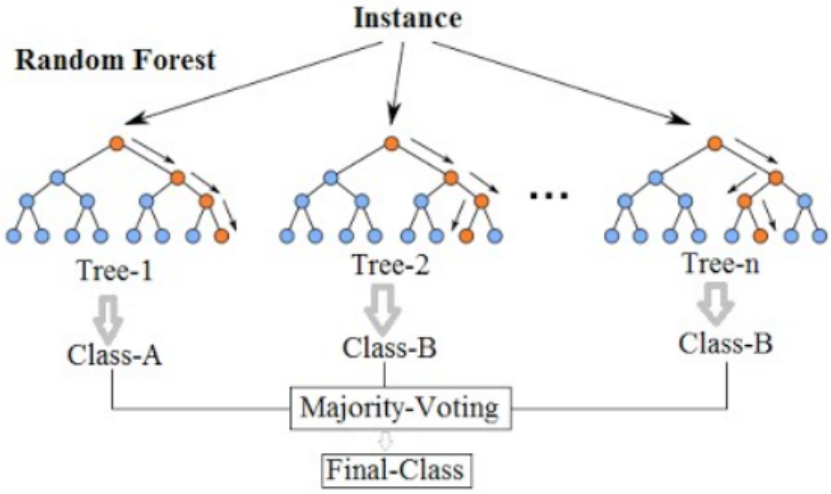

Figure 10. Random forest-based classification [18].

3.8. Ensemble Subspace KNN

The random subspace method works based on stochastic process. It picks various components randomly from the characteristic vector during the construction of each classifier as shown in Figure 11. For the nearest neighbor classifiers (KNN), a sample test is compared with a prototype, that provides the selected characteristics only that have contribution other than zero to the distance. From a geometric point of view, this is equivalent to projecting all points in the selected subspace and the closest neighbors k are calculated by the projected distances. A new set of k closest neighbors is calculated by selecting a random subspace every time. Nearest neighbors k in every selected subspace meet for a majority vote in the membership class test sample. If closest neighbor k is selected more times, this obtained the same training samples that appear more times in the set than once.

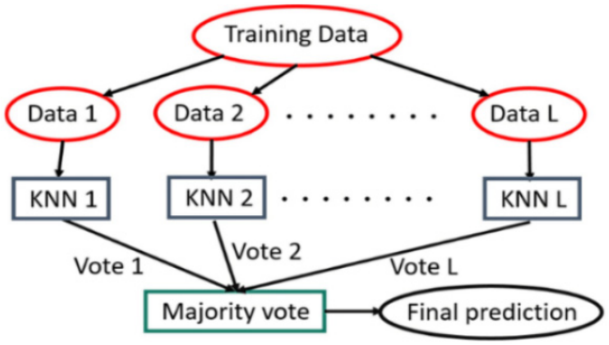

Figure 11. The ensemble (subspace KNN) [21].

Formally, given a set of N points in an n-dimensional feature space

$$\{(x_1, x_2, \ldots, x_n) | x_i \text{ is real for all } 1 \leq i \leq n\}$$

the m-dimensional subspaces

$$\{(x_1, x_2, \ldots, x_n) | x_i = 1 \; for \; i \in I, x_i = 0 \; for \; i \notin I\}$$

where I is a subset of elements m of {1,2, . . . , n} and m < n. In each step, a subspace is chosen by randomly selecting an I from C (n, m). All points are projected onto the chosen

subspace. For each test point, past KNN (k nearest neighbors) (1 < k 1), the test point is assigned to the class that has the most frequent incidences in list C.

$$\hat{F} = F\text{argmin}_{F} E_{x,y}[L(y, F(x))]$$

4. Results and Discussion

In this research, the behavior of four hand gestures including the stationary, double tap, single finger movement and finger spread were observed to understand attributes and features of hand movements for male and female subjects using a number of classifiers. Different classification approaches named as LDA, QDA, SVM, NN, ensemble (bagged tree), random forest, gradient boosted, and subspace KNN were adopted in our case to utilize and classify the hand movements.

In the experimental procedure, a total of four gestures were performed per trial of different subjects of different age groups (25–55 yr). The two groups were classified as male and female. For the male group, each subject performed all four gestures in a sequence of stationary, double tap, single finger movement and finger spread. Performing window of each gesture was selected of 1 min duration. Therefore, the proposed MYO based embedded system took data of 4 min for completion of each set of movements for a single subject. The same procedure was followed for extracting data in the case of the female group.

To employ the classification approach, we used the 5-fold cross-validation technique in our model of classify learner with four classes of EMG data. In the case of WEKA, 10-fold cross-validation approaches are used to classify our EMG data as shown in Figure 12. The scatter plot of four classes of EMG signals in classify learner is shown in Figures 13 and 14 where we can see the scatter plot of EMG data among each channel of MYO (as column 1 = channel 1, column 2 = channel 2, and so on) for both cases of male and female (As VarName 3 = channel 1, VarName 4 = channel 2, and so on). In our model of classify learner, we defined a response variable to classify the predictive behavior of four classes of EMG signal. For this reason, we marked our four-class hand gestures as 0 for stationary, 1 for double tap, 2 for movement of single finger and 3 for finger spread as response variable as shown in Table 1.

=== Detailed Accuracy by Class ===

	TP Rate	FP Rate	Precision	Recall	F-Measure	MCC	ROC Area	PRC Area	Class
	0.939	0.038	0.912	0.939	0.925	0.893	0.984	0.948	Stationary
	0.526	0.040	0.667	0.526	0.588	0.538	0884	0.626	Double Tap
	0.866	0.076	0.827	0.866	0.846	0.779	0.954	0.920	Single Finger
	0.833	0.070	0.818	0.833	0.825	0759	0.961	0.898	Finger Spread
Weighted Avg	0.833	0.059	0.828	0.833	0.829	0.775	0.955	0.883	

Confusion Matrix

a	b	c	d	←			Classified as
476	12	10	9	|	a	=	Stationary
21	120	40	47	|	b	=	Double Tap
24	13	439	31	|	c	=	Single Finger
1	35	42	390	|	d	=	Finger Spread

Figure 12. Classification results of WEKA.

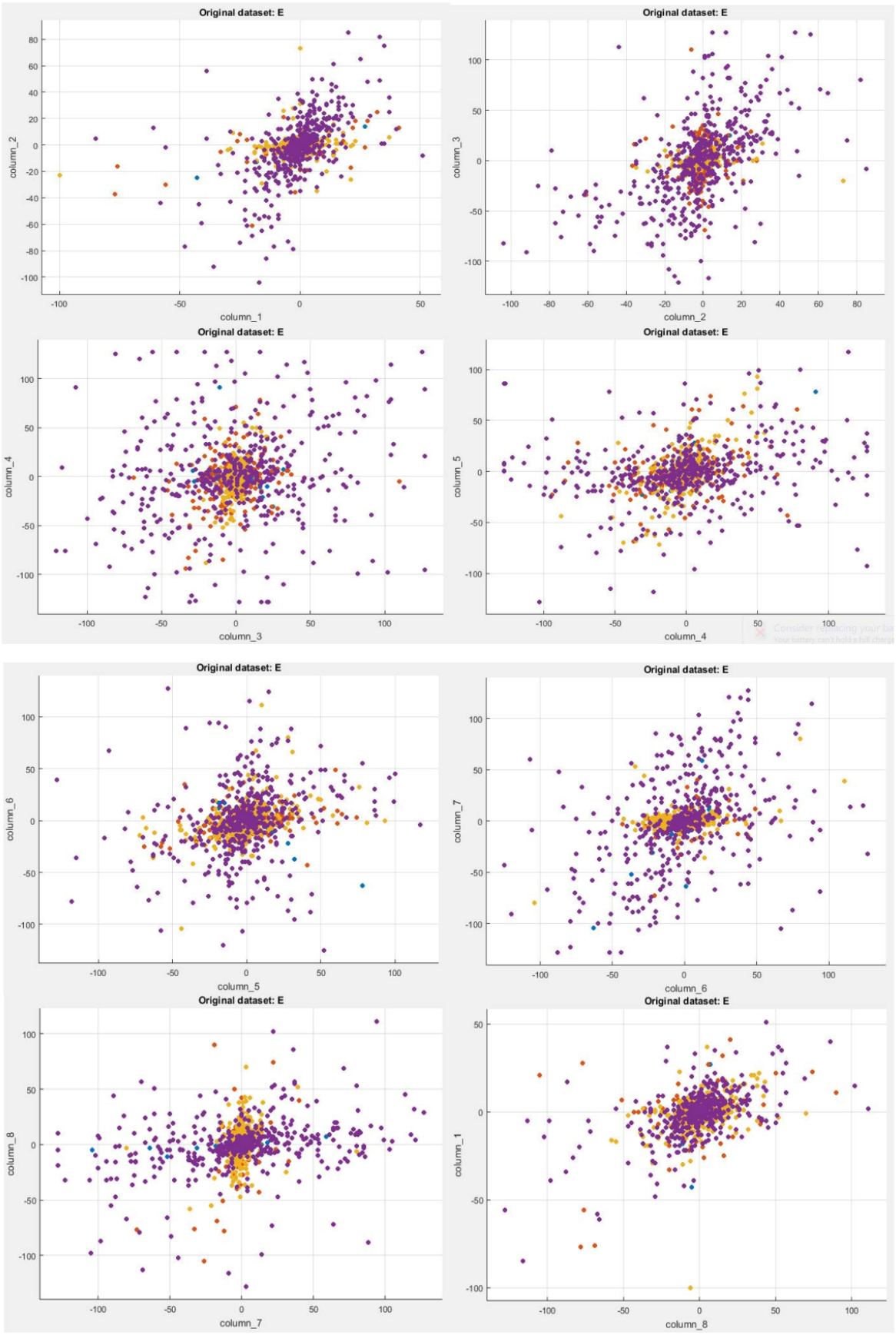

Figure 13. The eight−channel EMG scatter plot for males.

Figure 14. The eight−channel EMG scatter plot for females.

Table 1. The four classes of hand gestures.

Sr No.	Gesture	Nomination
1	Stationary	0
2	Double tap	1
3	Single finger movement	2
4	Finger spread	3

The results of this experiment show a high rate of accuracy with F-measure, MCC, and ROC. As from the results, we concluded that the ensemble bagged tree shows a higher rate of accuracy for both male and female subjects among the listed classifiers with 83.9% and 78.4%, respectively, as given in Tables 2 and 3.

Table 2. The performance results of classification (for males).

Sr No.	Classification Algorithm	Performance
1	QDA	72.4%
2	Quadratic SVM	82.6%
3	Fine Gaussian SVM	80.1%
4	Random forest	83.3%
5	Gradient boosted (tree)	81.2%
6	Ensemble (bagged tree)	83.9%
7	Ensemble (subspace KNN)	80.4%

Table 3. The performance results of classification (for females).

Sr No.	Classification Algorithm	Performance
1	QDA	69.4%
2	Quadratic SVM	72.2%
3	Fine Gaussian SVM	62.5%
4	Random forest	75.5%
5	Gradient boosted (tree)	71.2%
6	Ensemble (bagged tree)	78.4%
7	Ensemble (subspace KNN)	70.1%

Figures 13 and 14 demonstrate the real time scatter plot of EMG data acquired from the MYO armband. In this figure plot, four colors represent the four classes (stationary, double tap, single finger movement and finger spread) for a complete set of movements by a single subject.

The colors of related gestures are classified as

- red: stationary;
- blue: double tap;
- yellow: single finger movement;
- purple: finger spread.

Figures 13 and 14 present a set of eight subgraphs which represent the performance of each sensor of MYO with the other. As the MYO armband consists of eight EMG sensors, the given figures describe the behavior of all eight sensors with each other. Refer to Results and Discussion block (Column 1 = Channel 1, Column 2 = Channel 2 etc.). The dominance of different colors shows the action potential of muscles during each movement. For example, Figure 13 shows the maximum dominance of purple color which means that muscle concentration maximizes with finger spread as compared to other gesture movements.

The confusion matrix and ROC curve for both cases (male and female) are shown in Figure 15. The recognition rate of various hand movements after classification gives 92% for stationary, 68% for double tap, 83% for single finger movement and 82% for finger

spread gesture in male movement as shown in Figure 15a. While in the case of random forest for males, it gives the recognition accuracy for each gesture as 91% for stationary, 67% for double tap, 83% for movement of single finger and 82% for finger spread as given in Table 4.

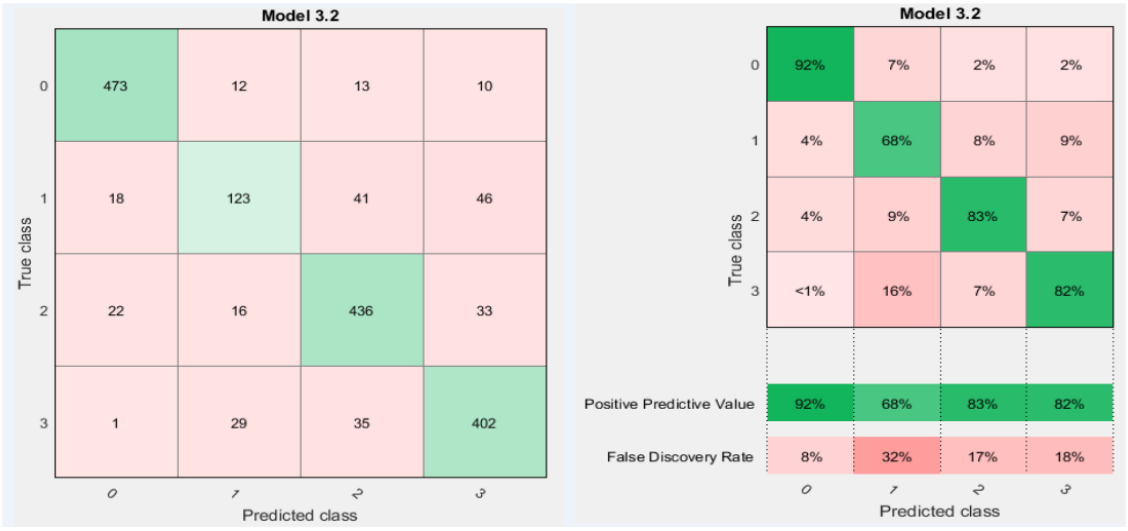

(**a**)

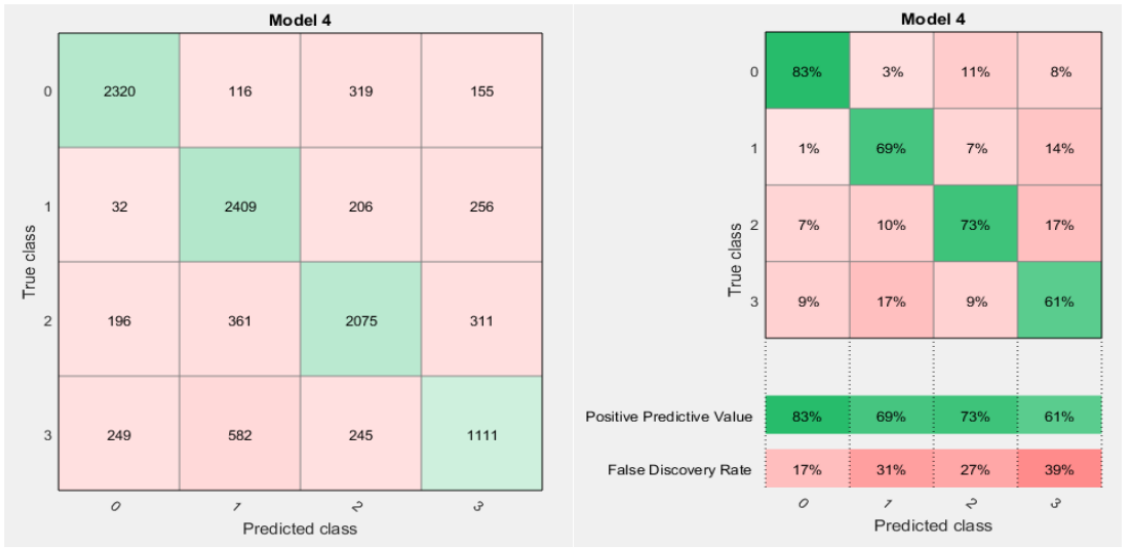

(**b**)

Figure 15. Confusion matrices of four-class hand gesture for females. (**a**) For males; (**b**) for females.

Table 4. Recognition rate for hand gestures.

Classification Algorithm	Stationary	Double Tap	Single Finger Movement	Finger- Spread
Ensemble (bagged tree)	92%	68%	83%	82%
Random forest	91%	67%	83%	82%

The recognition rate of hand movements in the female test case after classification gives up to 83% for stationary, 69% for double tap, 73% for single finger movement and 61% for finger spread gesture as shown in Figure 15b.

The region of convergence (ROC) curve was used to find the quality and accuracy of the running classifier. The marker on the plot exhibits the performance of the classifier as it shows the true positive rate (TPR) and false positive rate (FPR) of the running classifier

as shown in the Figures 16 and 17. For example, if it states the behavior of false positive rate (FPR) as 0.25 then it means that the classifier picks the 25% incorrect observations for the positive class. In turn, if the true positive rate (TPR) signifies the behavior of classifier as 0.75 then actually it shows that the classifier picks 75% correct observations for the positive class.

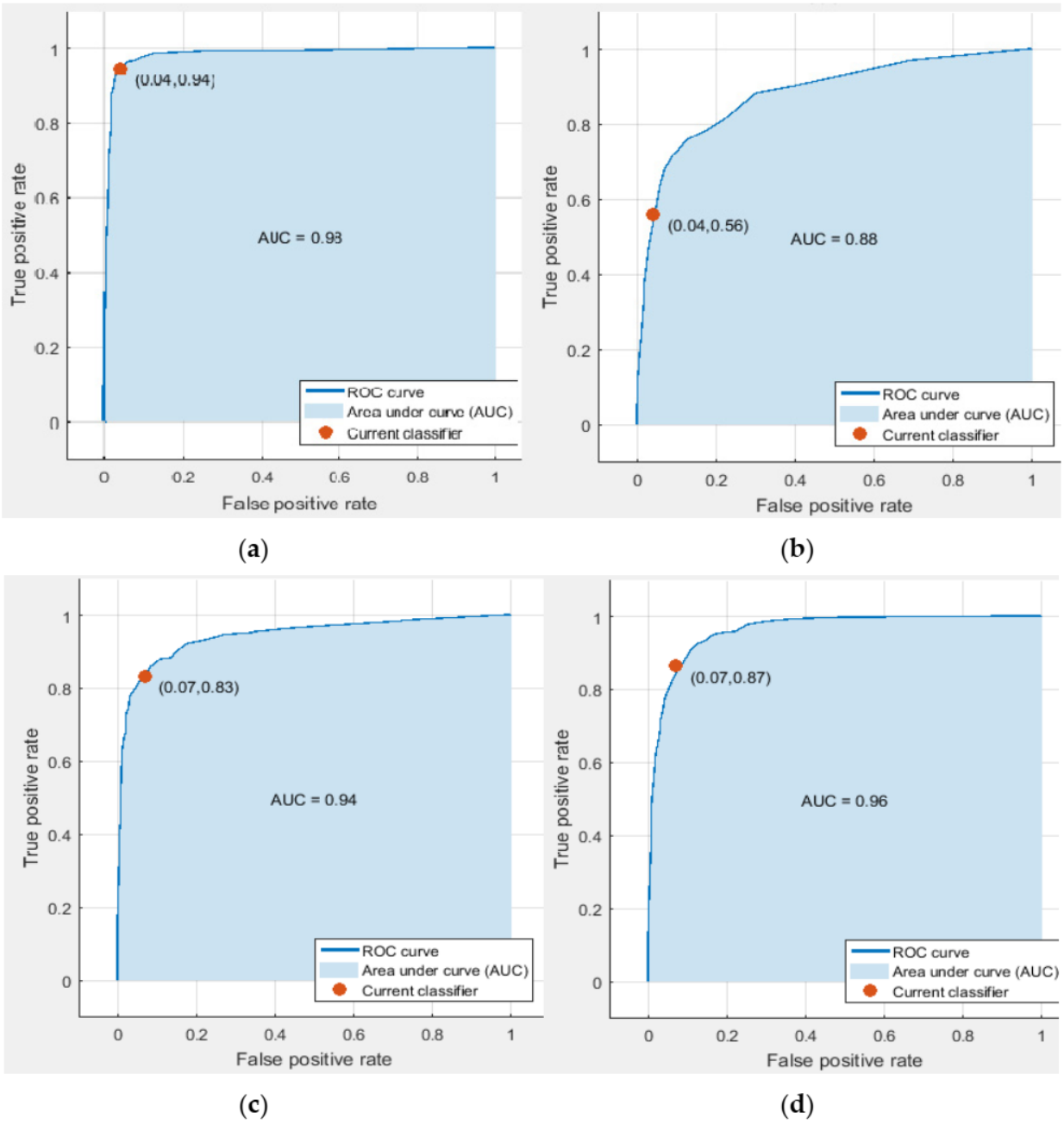

Figure 16. ROC curve of four classes of EMG data (for males): (**a**) stationary, (**b**) double tap hand gesture, (**c**) single finger movement, and (**d**) finger spread hand gesture.

In Figure 16, the top left corner with the right angle of the curve represents the perfect results with no misclassification rate. While, the point that lies with 45 degrees of curve line shows the poor results of classification. The AUC (area under the curve) is the measurement of recognition, classification, and quality of classifier results. A large area under the curve (AUC) represents the superior results of classification while the small area under curve indicates the inferior performance of classifiers.

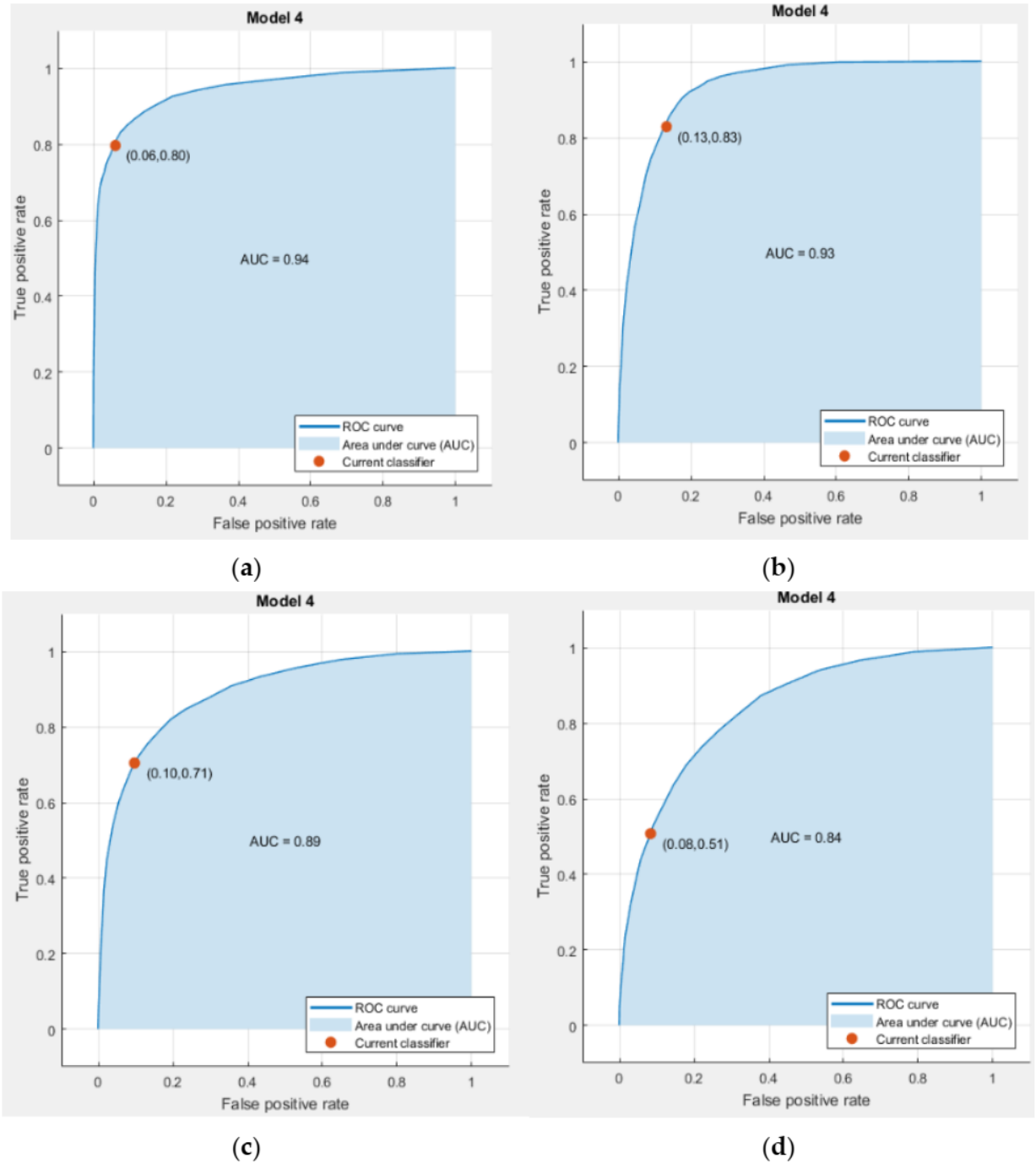

Figure 17. ROC curve of four classes of EMG data (for females): (**a**) stationary, (**b**) double tap hand gesture, (**c**) single finger movement, and (**d**) finger spread hand gesture.

Comparative Analysis

In the field of biomedical engineering, various design techniques and approaches have been used to develop efficient and cost-effective solutions for handicaps. For this purpose, some developers use invasive electrodes on muscles to acquire EMG data and some give preference to noninvasive design techniques through a controller or DAQ board. MYO armband is the latest approach and has become very widely used in a number of studies. As it is mentioned above in the literature that although previous design techniques improve the results of accuracy and reduce the cost of prosthetic design, it still requires some improvement in the cost of design.

The detailed comparison of different approaches with our proposed approach is given below in Table 5. As compared to previous approaches, we gave an idea of the MYO armband as a motion device for various upper limb movements through an embedded system and an external Bluetooth module with a good performance classifier. The overall system developed in the proposed case is relatively cheaper, noninvasive and gives good performance too compared to other costly systems with a high rate of accuracies. Moreover, the previous approaches used the surface EMG electrodes and sensors to capture data for upper limbs which comprises many obstructions such as motion artifacts, electromagnetic resonance of wires, signal to noise ratio and the most prominent of them is an invasive approach that quite painful for subjects.

Table 5. Comparison of different approaches used for classifying hand movements with the proposed approach.

Paper Ref.	Technique/Apparatus	Gestures/Purpose	Classifiers	Accuracy
[3]	11 electromagnetic sensors on a glove	Free hand movement,	Using GUI to explore gesture in real-time	NA/just connecting of a prosthetic hand
[12]	Five noninvasive surface electrodes	Three movements/upper arm flexion and extension, forearm pronation and supination and palmar flexion and dorsiflexion	AR model, backpropagation neural networks (BPNN)	81%
[13]	Three dimensional (3D) printed prosthesis with MYO	To provide an affordable, practical, and convenient solution for amputees	NA	NA
[14]	MYO armband	To control virtual robotic arm generated in unity 3D	NA	NA
[15]	Six pairs of surface electrodes (Ag/AgCl)	Nine gestures/wrist flexion, wrist extension, thumb close, making a fist, fingers spread, four-finger close, forearm supination, forearm pronation, open, and no motion	LDA and SVM (WT/SVM-OVO)	92.3%
[18]	Six surface EMG sensors	Three grasping things (mug, marker, rectangle) at three different places to observe	LDA, QDA, SVM, ANN, KNNand random forest	83%
[19]	Eight surface EMG sensors located on the forearm	Six gestures/wrist flexion, wrist extension, hand supination, hand pronation, hand opening, and hand closing	Discrete wavelet transform (DWT) of EMG signals with an unconstrained parameterization of mother wavelet using SVM to classify	5% misclassification rate
[20]	Surface electrodes with DAQ board and 16-bit A/D converter	59 person data with 19 normal, 20 myopathy patient and 20 neuropathy patients to classify	MLP and SVM under the supervision of PCA and FFT to enhance the accuracy	85.4%
[21]	MYO armband with Bluetooth using MEX file bridging with (laptop)	Nine subjects walking, running, resting and open door (to check wandering), a disease	SVM, naïve bias and KNN	More than 90%
[22]	MYO with help of Apple map connector (App)	Zooming, focusing and panning the map navigation using five gestures of MYO (fist, the finger spread, wave in, wave out and double tap)	Questionnaire-based study	NA
[39]	Multiscale principle component analysis surface EMG sensors	Normal, myopathy, ALS (types of muscles to detect) to classify data of these muscles	C4.5, CART and random forest decision tree	96%
[40]	Low-cost passive sensors, an innovative analog front-end system and low power microcontroller	Six gestures/power grip, precision grasp, open hand, pointed index and flexion/extension of the wrist	LDA, ANN, and SVM	92%
proposed	MYO armband/embedded controller/HM-10 Bluetooth module	Four gesture movements include stationary, double tap, single finger movement and finger spread	QDA, SVM, ensemble (bagged tree), gradient (boosted tree), random forest, ensemble (subspace KNN)	83.9%

We classified the four basic and general hand movements to study the liability of our system. The results of this study show comparatively good performance in detecting four hand movements with an accuracy of more than 80–92%. Moreover, this study can be used in the future to develop a cheap prosthetic design for an amputee.

5. Conclusions and Future Work

The aim of this research paper was to classify and recognize the hand movements for various upper limb movements. For this purpose, a novel method was proposed to acquire the EMG signals from forearm muscle with the MYO gesture control system on an embedded platform through a Bluetooth module. For getting different hand gestures, a total of 10 healthy subjects (five males and five females) participated in this research work. After acquiring EMG data from these participants, five-fold cross-validation approaches were used to classify these hand movements. The results based on classification using ensemble (bagged tree) gave a high rate of accuracy among other classifiers with a better recognition rate for various hand movements.

The results of this study can also be used in the future to develop an efficient, cost-effective and flexible assistive device or prosthesis. This work will also be extended to more or other gesture classification, as per need, based on same framework.

Author Contributions: Conceptualization, methodology, software, validation, H.A.J.; writing—original draft preparation, writing—review and editing, M.T.R., S.A.; visualization, supervision, M.I.T.; project administration, funding acquisition, J.I., A.A.; formal analysis, F.A.A. All authors have read and agreed to the published version of the manuscript.

Funding: This research was supported by National Centre of Robotics and Automation (NCRA) under Robot Design and Development Lab (RDDL), College of Electrical and Mechanical Engineering, NUST Islamabad, Pakistan. This research was funded by Higher Education Commission of Pakistan under grants titled "Establishment of National Centre of Robotics and Automation" (DF-1009-31).

Informed Consent Statement: Informed consent was obtained from all subjects involved in the study.

Acknowledgments: The authors are grateful to the College of Electrical and Mechanical Engineering, National University of Sciences & Technology, Islamabad and also to the Deanship of Scientific Research, King Saud University for funding through Vice Deanship of Scientific Research Chairs.

Conflicts of Interest: The authors declare no conflict of interest.

References

1. Li, G.F.; Jiang, D.; Zhou, Y.L.; Jiang, G.Z.; Kong, J.Y.; Manogaran, G. Human lesion detection method based on image information and brain signal. *IEEE Access* **2019**, *7*, 11533–11542. [CrossRef]
2. Qi, J.X.; Jiang, G.Z.; Li, G.F.; Sun, Y.; Tao, B. Intelligent human-computer interaction based on surface EMG gesture recognition. *IEEE Access* **2019**, *7*, 61378–61387. [CrossRef]
3. Shah, S.A.; Tahir, A.; Ahmad, J.; Zahid, A.; Pervaiz, H.; Shah, S.Y.; Ashleibta, A.M.A.; Hasanal, A.; Khattak, S.; Abbasi, Q.H. Sensor Fusion for Identification of Freezing of Gait Episodes Using Wi-Fi and Radar Imaging. *IEEE Sens.* **2020**, *20*, 14410–14422. [CrossRef]
4. Li, G.F.; Wu, H.; Jiang, G.Z.; Xu, S.; Liu, H. Dynamic gesture recognition in the internet of things. *IEEE Access* **2019**, *7*, 23713–23724. [CrossRef]
5. Huang, L.; Fu, Q.; Li, G.; Luo, B.; Chen, D.; Yu, H. Improvement of maximum variance weight partitioning particle filter in urban computing and intelligence. *IEEE Access* **2019**, *7*, 106527–106535. [CrossRef]
6. Cheng, W.; Sun, Y.; Li, G.; Jiang, G.; Liu, H. Jointly network: A network based on CNN and RBM for gesture recognition. *Neural Comput. Appl.* **2019**, *31*, 309–323. [CrossRef]
7. Li, X.; Zhou, Z.; Liu, W.; Ji, M. Wireless semg-based identification in a virtual reality environment. *Microelectron. Reliab.* **2019**, *98*, 78–85. [CrossRef]
8. Karabulut, D.; Ortes, F.; Arslan, Y.Z.; Adli, M.A. Comparative evaluation of EMG signal features for myoelectric controlled human arm prosthetics. *Biocybern. Biomed. Eng.* **2017**, *37*, 326–335. [CrossRef]
9. Jiang, D.; Li, G.F.; Sun, Y.; Kong, J.Y.; Tao, B. Gesture recognition based on skeletonization algorithm and CNN with ASL database. *Multimed. Tools Appl.* **2019**, *78*, 29953–29970. [CrossRef]
10. Jo, I.; Park, Y.; Lee, J.; Bae, J. A portable and spring-guided hand exoskeleton for exercising flexion/extension of the fingers. *Mech. Mach. Theory* **2019**, *135*, 176–191. [CrossRef]
11. Park, S.-Y.; Kim, S.-H.; Park, D.-J. Effect of slope angle on muscle activity during variations of the Nordic exercise. *J. Exerc. Rehabil.* **2019**, *15*, 832. [CrossRef]
12. Sapienza, S.; Ros, P.M.; Guzman, D.A.F.; Rossi, F.; Terracciano, R.; Cordedda, E.; Demarchi, D. On-line event-driven hand gesture recognition based on surface electromyographic signals. In Proceedings of the 2018 IEEE International Symposium on Circuits and Systems (ISCAS), Florence, Italy, 27–30 May 2018; pp. 1–5.

13. Pitou, S.; Wu, F.; Shafti, A.; Michael, B.; Stopforth, R.; Howard, M. Embroidered electrodes for control of affordable myoelectric prostheses. In Proceedings of the 2018 IEEE International Conference on Robotics and Automation (ICRA), Brisbane, Australia, 21–25 May 2018; pp. 1812–1817.
14. Ganiev, A.; Sin, H.S.; Lee, K.H. Study on virtual control of a robotic arm via a Myo armband for the self manipulation of a hand amputee. *Int. J. Appl. Eng. Res.* **2016**, *1*, 775–782.
15. Nastarin, A.; Akter, A.; Awal, M.A. Robust control of hand prostheses from surface EMG signal for transradial amputees. In Proceedings of the 2019 5th International Conference on Advances in Electrical Engineering (ICAEE), Dhaka, Bangladesh, 26–28 September 2019; pp. 143–148.
16. Shah, S.A.; Yang, X.; Abbasi, Q.H. Cognitive health care system and its application in pill-rolling assessment. *Int. J. Numer. Model.* **2019**, *32*, e2632. [CrossRef]
17. Masson, S.; Fortuna, F.S.; Moura, F.S.; Soriano, D.C. Integrating Myo armband for the control of myoelectric upper limb prosthesis. In Proceedings of the XXV Congresso Brasileiro de Engenharia Biomédica (CBEB), Foz do Iguaçu, Brazil, 17–20 October 2016; pp. 1–4.
18. Mendez, I.; Hansen, B.W.; Gravow, C.M.; Smedegaard, E.J.L.; Skogberg, N.B.; Uth, X.J.; Bruhn, A.; Geng, B.; Kamavuako, E.N. Evaluation of the Myo Armband for the Classification of hand motions. In Proceedings of the IEEE International Conference on Rehabilitation Robotics, London, UK, 17–20 July 2017; pp. 1211–1214.
19. Pancholi, S.; Joshi, A.M. Electromyography-based hand gesture recognition system for upper limb amputees. *IEEE Sens. Lett.* **2019**, *3*, 1–4. [CrossRef]
20. Raurale, S.A.; McAllister, J.; del Rincon, J.M. Real-time embedded EMG signal analysis for wrist-hand pose identification. *IEEE Trans. Signal Process.* **2020**, *68*, 2713–2723. [CrossRef]
21. Pizzolato, S.; Tagliapietra, L.; Cognolato, M.; Reggian, M.; Muller, H.; Atzori1, M. Comparison of six electromyography acquisition setups on hand movement classification tasks. *PLoS ONE* **2017**, *12*, e0186132. [CrossRef]
22. Cognolato, M.; Atzori, M.; Faccio, D.; Tiengo, C.; Bassetto, F.; Gassert, R.; Muller, H. Hand gesture classification in transradial amputees using the Myo armband classifier. In Proceedings of the 2018 7th IEEE International Conference on Biomedical Robotics and Biomechatronics (Biorob), Enschede, The Netherlands, 26–29 August 2018; pp. 156–161.
23. #MyoCraft: Arduino Projects with MyoDuino. Available online: http://developerblog.myo.com/myocraft-ardunio-projects-with-myoduino/ (accessed on 5 May 2021).
24. Gowtham, S.; Krishna, K.M.A.; Srinivas, T.; Raj, R.G.P.; Joshuva, A. EMG-based control of a 5 DOF robotic manipulator. In Proceedings of the 2020 International Conference on Wireless Communications Signal Processing and Networking (WiSPNET), Chennai, India, 4–6 August 2020; pp. 52–57.
25. Jia, G.; Lam, H.-K.; Liao, J.; Wang, R. Classification of electromyographic hand gesture signals using machine learning techniques. *Neurocomputing* **2020**, *401*, 236–248. [CrossRef]
26. Arozi, M.; Caesarendra, W.; Ariyanto, M.; Munadi, M.; Setiawan, J.D.; Glowacz, A. Pattern recognition of single-channel sEMG signal using PCA and ANN method to classify nine hand movements. *Symmetry* **2020**, *12*, 541. [CrossRef]
27. Toutountzi, T.; Collander, C.; Phan, S.; Makedon, F. EyeOn: An activity recognition system using MYO armband. In Proceedings of the 9th ACM International Conference on Pervasive Technologies Related to Assistive Environments, Corfu Island, Greece, 29 June–1 July 2016; p. 82.
28. Ding, J.; Lin, R.-Z.; Lin, Z.-Y. Service robot system with integration of wearable Myo armband for specialized hand gesture human–computer interfaces for people with disabilities with mobility problems. *Comput. Electr. Eng.* **2018**, *69*, 815–827. [CrossRef]
29. Toledo-Perez, D.C.; Rodriguez-Resendiz, J.; Gomez-Loenzo, R.A.; Jauregui-Correa, J.C. Support vector machine-based EMG signal classification techniques: A review. *Appl. Sci.* **2019**, *9*, 4402. [CrossRef]
30. Electromyography. Available online: https://en.wikipedia.org/wiki/Electromyography (accessed on 5 May 2021).
31. Lopes, J.; Simao, M.; Mendes, N.; Safeea, M.; Afonso, J.; Neto, P. Hand/arm gesture segmentation by motion using IMU and EMG sensing. In Proceedings of the 27th International Conference on Flexible Automation and Intelligent Manufacturing, FAIM2017, Modena, Italy, 27–30 June 2017.
32. Riaz, M.T.; Ahmed, E.M.; Durrani, F.; Mond, M.A. Wireless Android Based Home Automation System. *ASTES* **2017**, *2*, 234–239. [CrossRef]
33. Tavakoli, M.; Benussi, C.; Lourenco, J.L. Single channel surface EMG control of advanced prosthetic hands: A simple, low cost and efficient approach. *Expert Syst. Appl.* **2017**, *79*, 322–332. [CrossRef]
34. Ahmad, J.; Butt, A.M.; Riaz, M.T.; Bhutta, S.; Kham, M.Z.; Ul-Haq, I. Multiclass Myoelectric Identification of Five Fingers Motion using Artificial Neural Network and Support Vector Machine. *ASTES* **2017**, *2*, 1026–1033. [CrossRef]
35. Sathiyanarayanan, M.; Rajan, S. MYO armband for physiotherapy healthcare: A case study using gesture recognition application. In Proceedings of the 8th International Conference on Communication Systems and Networks (COMSNETS), Bangalore, India, 5–10 January 2016.
36. Krasoulis, A.; Vijayakumar, S.; Nazarpour, K. Multi-grip classification-based prosthesis control with two EMG-IMU sensor. *IEEE Trans. Neural Syst. Rehabil. Eng.* **2020**, *28*, 508–518. [CrossRef]
37. Tuncer, T.; Dogan, S.; Subasi, A. Surface EMG signal classification using ternary pattern and discrete wavelet transform based feature extraction for hand movement recognition. *Biomed. Signal Process. Control* **2020**, *58*, 101872. [CrossRef]

38. Arteaga, M.V.; Castiblanco, J.C.; Mondragon, I.F.; Colorado, J.D.; Alvarado-Rojas, C. EMG-driven hand model based on the classification of individual finger movements. *Biomed. Signal Process. Control* **2020**, *58*, 101834. [CrossRef]
39. Kańtoch, E. Recognition of sedentary behavior by machine learning analysis of wearable sensors during activities of daily living for telemedical assessment of cardiovascular risk. *Sensors* **2018**, *18*, 3219. [CrossRef]
40. Cao, T.; Liu, D.; Wang, Q.; Bai, O.; Sun, J. A wearable and portable real-time control gesture recognition system for bionic manipulator. *J. Phys. Conf. Ser.* **2020**, *1549*, 52060. [CrossRef]